Medical Physics
The International Journal of Medical Physics Research and Practice

Toward a unified view of radiological imaging systems

Robert F. Wagner, Kenneth E. Weaver, Earl W. Denny, and Robert G. Bostrom

Citation: Medical Physics **1**, 11 (1974); doi: 10.1118/1.1637272
View online: http://dx.doi.org/10.1118/1.1637272
View Table of Contents: http://scitation.aip.org/content/aapm/journal/medphys/1/1?ver=pdfcov
Published by the American Association of Physicists in Medicine

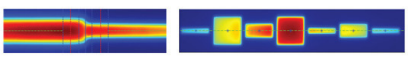

Toward a unified view of radiological imaging systems

Part I: Noiseless Images

Robert F. Wagner, Kenneth E. Weaver, Earl W. Denny, and Robert G. Bostrom

Division of Electronic Products, Bureau of Radiological Health, Rockville, Maryland 20852

A brief overview of the radiological imaging problem is presented, emphasizing the need for parametrizing components for the user, medical physicist, or system designer. Against this background a method is proposed for reducing MTF data. The single parameter obtained is analogous to criteria of "sharpness" used in other optical applications. The example of x-ray tube focal spots is examined in detail; results are presented and compared with other criteria. Finally, a prescription for cascading elements into a system is given and applied to the case of magnification radiography.

I. Introduction

Resolution gauges (bar targets) have long been used in the evaluation of imaging systems. However, it is well known that the upper limit of resolution (highest number of line pairs/mm resolvable) is not a good single criterion of image quality. In fact, it can be deceiving since two components with identical upper limits can behave quite differently from each other at lower spatial frequencies. For this reason the modulation-transfer function (MTF) is studied. This gives the percent contrast transfer from object to image as a function of spatial frequency.

With the MTF one has a continuous parametrization instead of a single parameter. This has the great advantage of being a more complete treatment; it also allows one to analyze system components in cascade since the MTF is just the component black-box transfer function and these simply multiply pointwise for linear elements in cascade to give an overall system MTF.

At this point, however, the analysis becomes more suited to a specialized laboratory and less accessible to the user. He might find more useful a *working* parameter for *estimating* the quality of the results he might expect from a given component or combination of components. One has some feel, for example, of what to expect when using what is referred to as a "one-millimeter focal spot." However, as will be discussed later, even this parameter is subject to ambiguity. There is a practical need to remove such ambiguity and provide the user with a parameter which will enable him to estimate what to expect from a given component (focal spot, intensifying screen, image intensifier, motion, scatter, etc.) and what to expect when combining components. This paper examines the possibility of deriving such a single parameter for the case where the image is *not noise limited.*

Section II reviews some general considerations concerning the use of screens and focal spots. Section III presents some data collected on x-ray tube focal spots in our laboratory to provide some examples for Sec. IV. In this latter section we introduce our method of analysis, together with its interpretation and some results. In Sec. V we show how this parametrization can be used for cascading imaging components and predicting overall system response, using the example of magnification radiography.

The emphasis on focal spots in this paper should be considered in the context of current practice: MTF data on screens is known to better than 10%—perhaps a few percent; attempts to quantify focal spots agree only to within a factor of 2! And, as is well known, the focal spot can often be the limiting component in an imaging system.

II. Generalities—screens and focal spots

If a point-source object, say a piece of lead with a fine hole in it, is radiographed in intimate contact with a film-screen

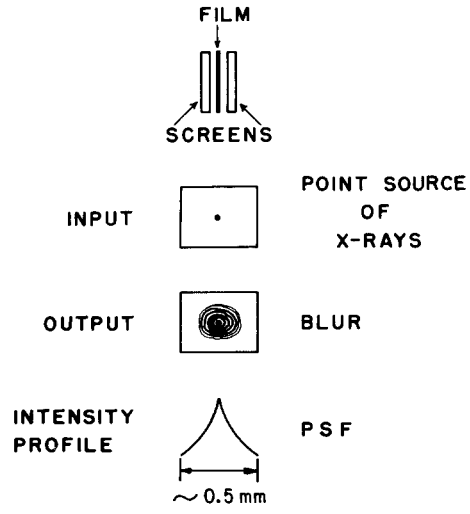

FIG. 1. Point Spread Function (PSF) for film-screen combination represented schematically—the point source is understood to be in contact with one of the screens.

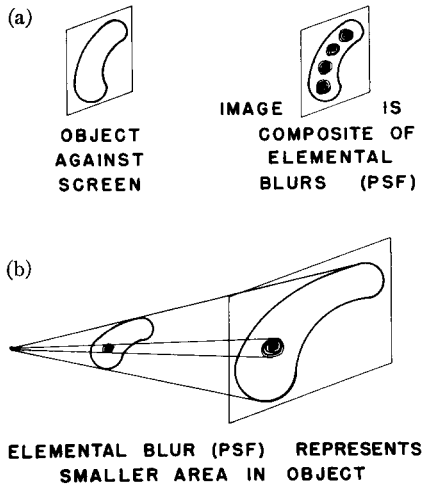

FIG. 2. Ideal (point) focal spot and a real screen–film combination: the object–image relation is represented schematically for the case of no magnification (a), and with magnification (b).

cassette, the resulting image is blurred by the diffusion of light in the screens. The intensity profile of the blur is called the point-spread function (PSF) (see Fig. 1). A more general object can be considered to be made up of a continuum of such point sources with varying transmissions. Its image is a composite of such elemental blurs (see Fig. 2, this composition is often referred to as the convolution of the object with the PSF). These blurs may destroy diagnostic information in the image. One may, however, try to regain lost information by going to magnification radiography.

If one has an ideal (point) source of x rays, then, in principle, one will gain by going to magnification. This follows from the fact that the elemental blurs in the image have the same size as they would without magnification, but they now represent a smaller area within the object (see Fig. 2).

Now let us consider imaging using a real focal spot and an ideal screen (no blur), or a very high resolution non-screen film. In this case if the object is not in contact with the cassette or film, the image again will be a composite of blurs. The elemental blurs will have the shape of the focal spot with the overall size determined by the geometry. This follows from the fact that the image or radiograph of a point in the object is just the pin-hole camera radiograph of the focal spot for the given geometry (Fig. 3). This is the PSF for the focal spot for the particular magnification.

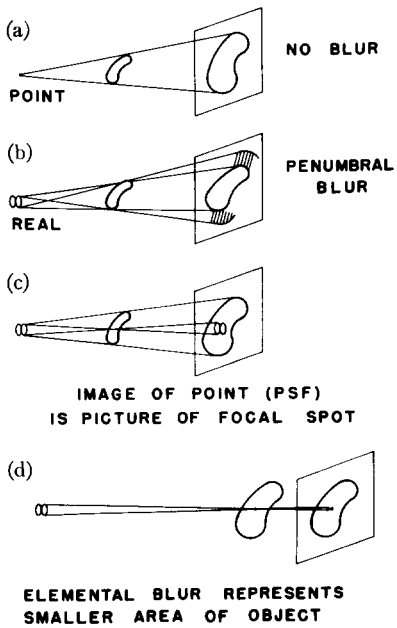

FIG. 3. Idealized image receptor combined with: Idealized focal spot (a); real focal spot emphasizing penumbral blur (b); real focal spot emphasizing image of a point within the object (c)—all under conditions of magnification. The effect of less magnification (d) is the opposite of that found with the idealized focal spot and a real image receptor (Fig. 2).

In this case, however, if one wants to try to regain information lost in the blurs, then *less* magnification is required (Fig. 3, bottom), unit magnification (intimate contact) being best in the case where the image receptor is perfect.

In the general case there is a trade-off between blurs due to the focal spot and to the screen—in a symmetric way. But before attempting to quantify the problem of the complete *system*, let us see what quantitative data exists for the *individual* components.

There exists a rather extensive literature on spread functions (and MTFs) for radiographic intensifying screens.[1–3] The data available on focal spots are somewhat more sparse, and many variables affect the gathering of these data.[4,5] We will present below some focal-spot data obtained in our laboratories; then we will proceed with suggestions on how these data may be used to fulfill the needs mentioned in the introduction.

III. Focal-spot intensity distributions

Many analyses of focal spots start from the assumption that the distribution is uniform over the surface of a square or rectangle. However, even though the actual non-uniformity had been documented as long ago as 1937 by Beese,[6] it is only quite recently that authors have emphasized that intensity distributions of actual focal spots fall somewhere between that of a rectangle and that of two parallel "hot" line sources.[5,7,8] Our data add a few nuances to what has already been observed. Figures 4(a) through 6(a) are three-dimensional displays of density traces of pin-hole camera radiographs of some focal spots of tubes in our laboratory. With the film and exposure conditions used, the density is proportional to x-ray intensity. The radiographs were made under the following conditions: Fig. 4 (a nominal 2-mm focal spot), 1:2 magnification; Figs. 5 and 6 (nominal 1-mm focal spots), 1:1 magnification; a 75-μm pin-hole was used with Kodak RP/M film. The films were scanned with a 40×40-μm aperture using a sampling interval of 40 μm.

A close inspection of Fig. 4(a) reveals the filament wires (the focal spot being very roughly an image of the cathode filament); Fig. 5(a) displays some severe departure from symmetry in both the x and y axes; and Fig. 6(a) displays a case of gradually sloping edges that would make a size determination by direct measurement somewhat arbitrary. All of the traces display the characteristic two-hot-line source distribution. Figures 4(b) through 6(b) are contour maps of lines of constant intensity (density) for the corresponding focal spots. These could be used if an edge criterion were of interest.

Another kind of data that we have been gathering and that has been found useful by many workers in this field

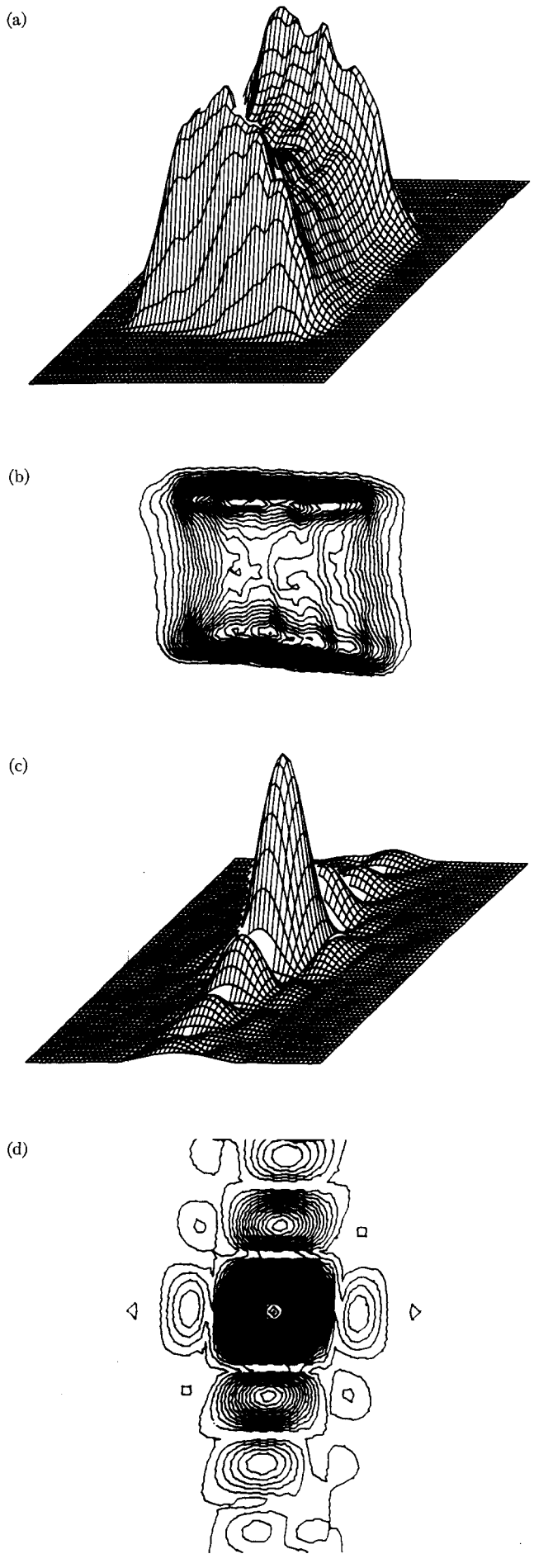

is the radiograph of the star or spoke target. Figure 8 is an example of such a radiograph. The periphery of the target represents low spatial frequencies (i.e., variation over relatively large distances) compared to the region near the hub, which represents relatively higher frequency spatial variations. Following a horizontal line through the center of the image from the outside into the center, one finds the familiar increase in blur until one reaches the so-called "disappearance frequency"; continuing toward the center there is renewed improvement in contrast in the region of "spurious resolution," i.e., resolution with 180° phase reversal—one finds a dark image line where a light one is expected and vice versa. This blurring and subsequent reversal can often be observed several times before the image is completely washed out near the hub. The first blur or disappearance frequency has been used to quantify focal spot size; we will return to this in Sec. IV.

A more quantitative representation of the above information is contained in the Fourier transform of the focal-spot intensity distribution. Whereas the PSF was a study of the elemental blur, and the spoke target was a study of a continuously varying target with a square wave distribution, the Fourier transform of the PSF is the predicted contrast transfer of a grid target with a sinusoidal variation. The MTF or absolute value of the Fourier transform of the focal-spot intensity distributions of Figs. 4(a) through 6(a) is shown in Figs. 4(c) through 6(c), respectively. The information displayed in such a representation is inverted with respect to the display in the image of the spoke target (that is, in the latter the contrast transfer of the lower spatial frequencies occurs at the periphery, and the higher frequencies near the center); in the Fourier transform representation shown here, the lower spatial frequencies occur in the center and the higher frequencies near the periphery of the representation.

One can see that the transfer falls off differently in different directions. The connection between a point on the MTF curve or surface and the orientation of a sine-wave grid whose contrast transfer is predicted is the following: The radius line from the center of the MTF curve to the point of interest is perpendicular to the lines of the grid.

The zeros or nulls of the MTF surface represent complete blurs and correspond to the so-called disappearance frequency on the image of the star or spoke target.

The Fourier transforms we have shown in Figs. 4(c) through 6(c) were obtained by means of a digital computer

FIG. 4. (a) Two-dimensional distribution of x-ray intensity from focal spot. The grid spacing is 40 by 40 μm. (b) Contour lines of constant intensity for focal spot distribution. (c) Two-dimensional MTF distribution for accompanying intensity distribution. The grid spacing is 0.13 lp/mm by 0.13 lp/mm (Fig. 4) or 0.1 lp/mm by 0.1 lp/mm (Fig. 5 and Fig. 6). The MTF's may be thought of as representing the transform in the plane of the focal spot itself. They can then be scaled to the object plane by the scale factor $M/(M-1)$, where M is the magnification. Notice that MTF information is on a scale that is basically the inverse of the intensity information scale; it is also distributed in directions that are perpendicular to the structures which generate it. (d) Contour lines of constant contrast transfer for MTF distribution.

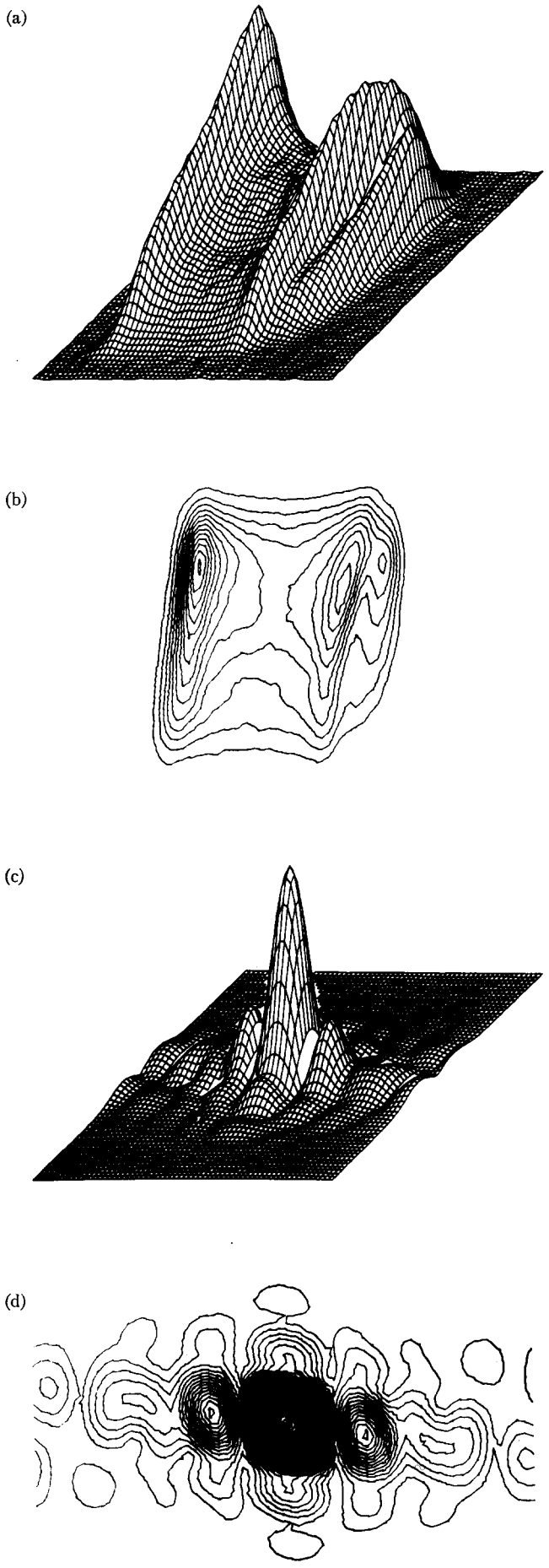

FIG. 5. See Fig. 4 caption and text for discussion.

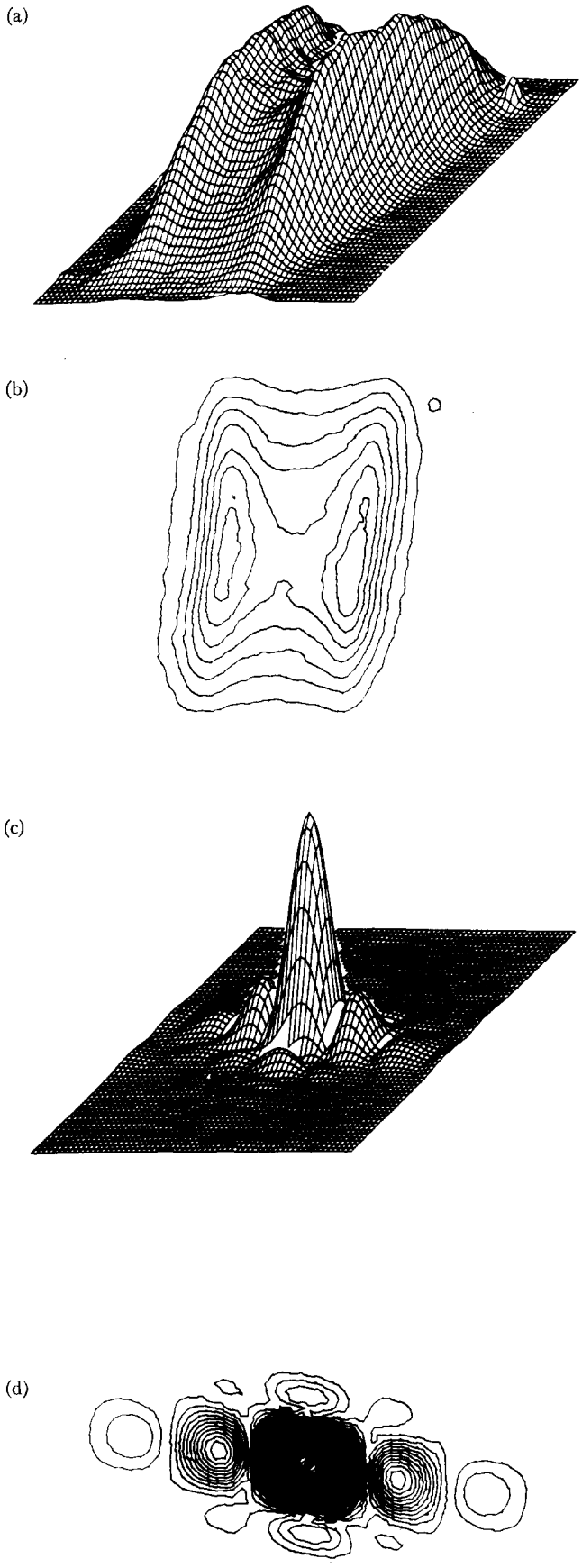

FIG. 6. See Fig. 4 caption and text for discussion.

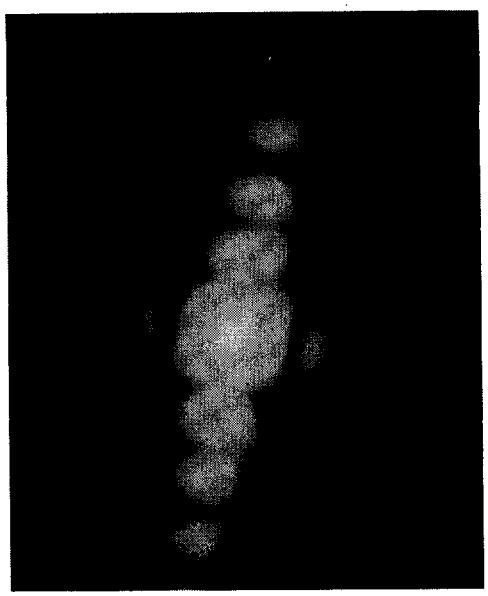

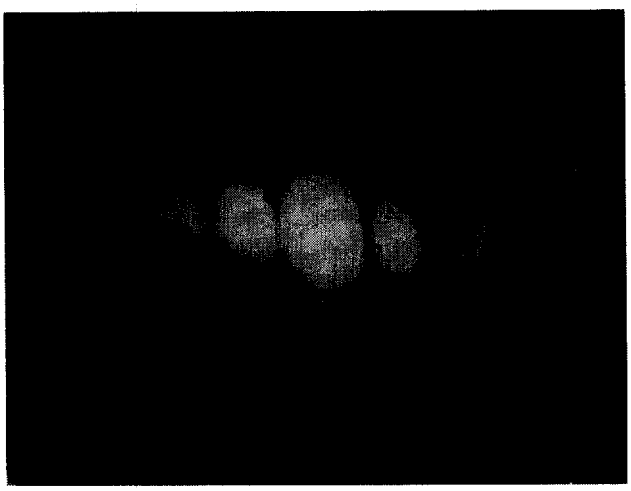

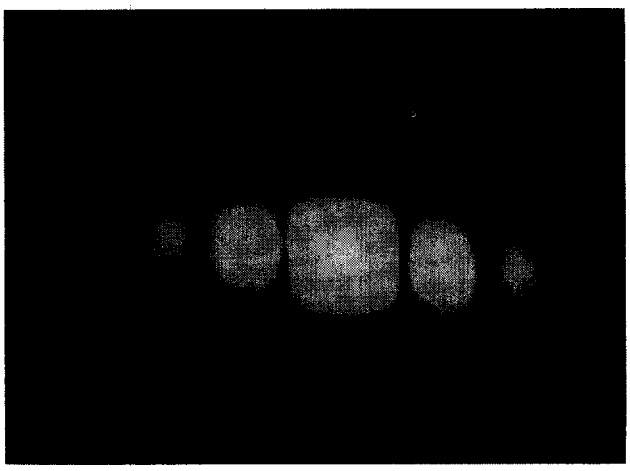

FIG. 7. Photographs of the far-field diffraction patterns of transparencies prepared from the pin-hole radiographs according to the prescription given in this paper. These patterns represent the MTF squared and may be compared qualitatively with the MTF contours of Figs. 4–6: (a) with Fig. 4(d); (b) with Fig. 5(d); and (c) with Fig. 6(d).

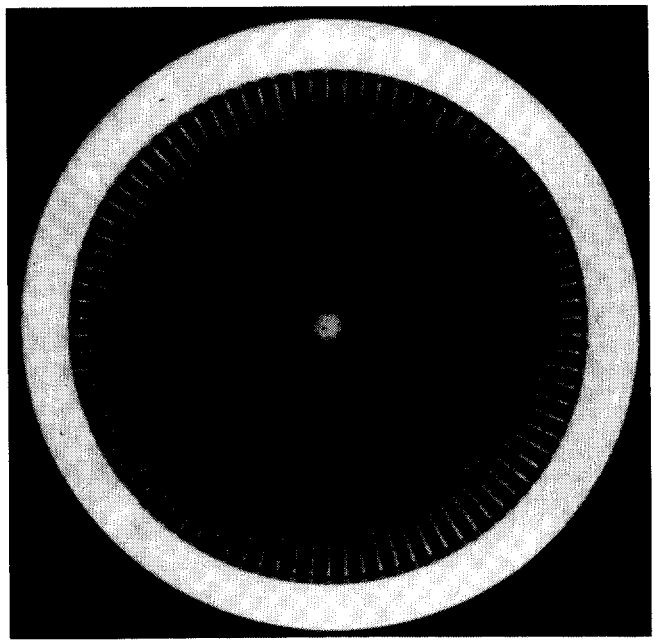

FIG. 8. Radiograph of the spoke target under conditions of 2× magnification showing the disappearance or first blur, followed by spurious resolution (moving horizontally from outside in), and a range of phase shifts (following a vertical bar—notice S-shaped wiggles).

from the intensity scans of the focal spot radiographs by a microdensitometer.[9] It is also possible to obtain the Fourier transform of an aperture, or the like, optically. The Fraunhofer or far-field diffraction pattern of an aperture illuminated with a plane, monochromatic, coherent wave is the Fourier transform of the aperture.[10] This result can be realized in a small space by using a laser, a pin-hole filter of the laser light, a converging lens, and a suitably prepared transparency (see Fig. 9).

Pin-hole camera radiographs of focal spots are "negatives"; if they are placed in the sample plane shown in Fig. 9, the transform will be degraded by (convolved with) the transform of the aperture that defines the laser beam at the transparency; in addition, one would be transforming the additional noise surrounding the focal-spot image. The next step, then, is to prepare a positive transparency of the image of the focal spot. One would like this transparency to pass laser light in proportion to the intensity distribution of the x rays from the focal spot. This can be done using a trick that is common in the photographic industry.

If a negative image is prepared on a film with a gamma of γ_1, [gamma is the slope of the density versus log exposure (H & D) curve, considered constant for the given relationship to hold] and the image is transferred to a film with a gamma of γ_2, the transmission of laser-light amplitude will be proportional to the original exposure of the first film if $\gamma_1\gamma_2 = 2/Q$, where Q is the Callier coefficient of the second film (ratio of specular density to diffuse density).

We tried using this approach playing the linear portions of various combinations of H & D curves off against one another. The resulting positive transparencies allowed too much transmission of laser light in the periphery (i.e., the background density was too low), and the transforms had some of the artifacts mentioned above. It was decided to

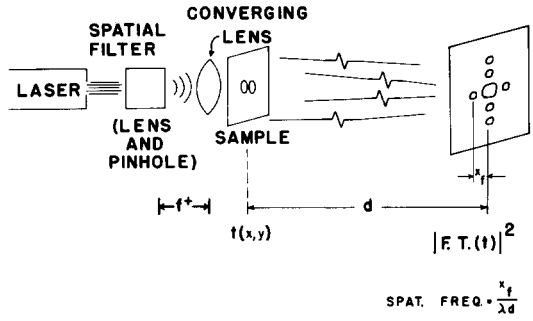

FIG. 9. Schematic of a simple system for performing a Fourier transform optically: f^+ is a distance slightly greater than the focal length of the converging lens; t is the transmission distribution in the sample plane; d is the distance from the sample plane to the transform plane (in our case, of the order of 10 m); x_f is a coordinate in the frequency or transform plane; and λ is the wavelength of the laser light.

generalize the above approach. This involved using the nonlinear portions of the H & D curve of two films closer to the toe. A program was developed to give complete freedom of adjustment of relative exposures and to allow playing the nonlinear portions off against one another in such a way as to make the overall transmission of laser amplitude proportional to original x-ray intensity. Some results are shown in Fig. 10. A small toe of non-linearity results [Fig. 10(d)]; the non-linear shoulder is avoided in practice by holding the maximum density of the original exposure below that point.

A qualitative comparison between Fourier transforms obtained optically from transparencies prepared as just discussed and those obtained digitally can be made by comparing Figs. 7(a), 7(b), and 7(c), with Figs. 4(d), 5(d), and 6(d) (the latter being the contours of the respective MTF surfaces). The qualitative agreement is striking. A quantitative comparison is yet to be made, but as will appear later in this paper, quantification of the optical results constitutes an important segment of our future plans. It will mean that the parameters discussed in this paper can be obtained with a simple optical system, without recourse to a computer or elaborate microdensitometer.

We have gathered complete intensity and Fourier-intensity distributions for a number of x-ray tubes at various technique factors. Several characteristics peculiar to these distributions that distinguish them from the ideal, uniform focal spot presupposed in much of the literature should be noted: (1) As shown by Rao and Bates[5] and Gray,[8] the onset of spurious resolution occurs at a lower frequency for such two-humped distributions than it would for a uniform square of the same outside dimensions. This makes the two-humped distribution equivalent to a square of *larger dimensions*. (2) The lack of symmetry in the intensity distributions gives rise to sine components in the MTF—in general, arbitrary phase shifts are possible (see, for example, the curving S-shaped bars in Fig. 8); this also has been studied by Rao and Bates.[5]

Before suggesting how these data might be reduced, we will introduce the intuitive idea of the so-called "sampling aperture"—a concept which may be helpful in bringing together the idea of the blur and the transfer function; this concept offers the most meaningful and useful one-parameter reduction of the data that we have found.

IV. Analysis and interpretation

Sampling aperture

An important and useful concept in optics is that of the "sampling aperture." A good example for introducing the idea is the case of a microdensitometer with "excellent" optics compared to the dimensions of the slit or other aperture used. The slit takes a sample from an area equal to its image at the film. This sample area is actually integrated over or averaged. It effectively smears the sample out over that area. That area is then, in effect, the point spread function for the optical system (if the remaining optics are "perfect"). A point source of transmission on the film is read as though it were distributed over this area.

Applying this concept to the phenomenon of spurious resolution helps tie together the concepts of "smearing" or blurring and contrast transfer. Figure 11(a) shows a sinusoidal transmission distribution sampled by a window or aperture that is equal to three half-wavelengths in length. When the aperture is centered over a point that is *negative* (with respect to the mean) it averages two positive half cycles with one negative half cycle. The result is a *positive* quantity (with respect to the mean) and vice versa when centered over a positive hump. In this way the sample turns out to be 180° out of phase with the object (i.e., the contrast transfer is negative). If one pursues this approach for varying wavelengths one is simply generating the Fourier transform of the aperture or the MTF, neglecting phase (for example, when the aperture is equal to one wave-

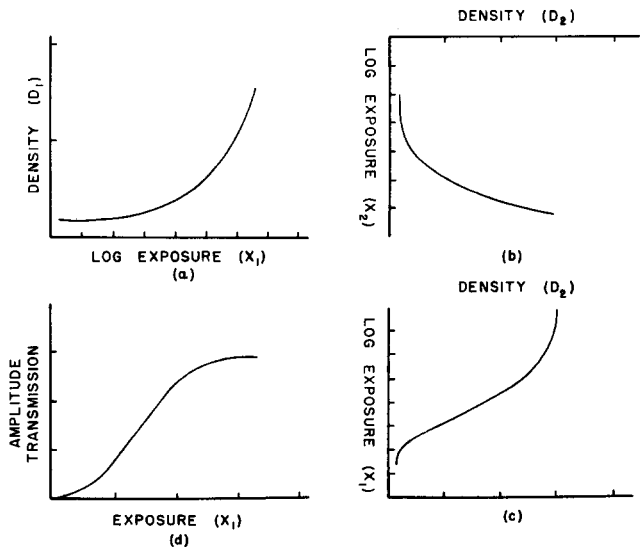

FIG. 10. (a) H & D curve of film (Kodak RP/M) used in making pinhole radiograph—each density interval is 1.0 density units, each log exposure interval is 0.3 (a doubling of exposure). (b) H & D curve of film (Kodak Single Emulsion Type R) used to make a positive contact print of the pinhole radiograph. The exposure X_2 to this film is just the transmission through the first film (a). (c) Density (D_2) of the positive vs log exposure (X_1) of the pinhole radiograph. (d) Amplitude transmission of laser light versus x-ray focal spot exposure (X_1) distribution. Full scale along the transmission axis is 100%. Arbitrary units are used along the exposure axis.

length, the average sample taken is equal to the mean: zero contrast transfer—the disappearance frequency).

The focal spot of an x-ray tube is a sampling aperture in the above sense. This is illustrated for a one-dimensional, uniform focal spot in Fig. 11(b). The image at a point P on the film is the average of all of the sample subtended by rays from the focal spot to that point, as illustrated (the solid line represents the actual intensity pattern). This piece of the sample can be called the effective sampling aperture of the focal spot. (It is clearly a function of the geometry or magnification used.) It represents the spread function of the focal spot in the object plane.

In general, however, we have seen that focal spots do not have a uniform intensity distribution, and they are obviously not one dimensional. The effective sampling aperture concept must then be generalized to cover the practical case. This generalization utilizes a two-dimensional version of the concept of "equivalent passband" which was introduced by Otto Schade[11] to study television systems. It will give rise to an effective sampling aperture that represents an average smear or blur size. (Schade's one-dimensional treatment, including some of the elements introduced below, was introduced to radiography by Russell Morgan,[12] but does not appear to have been fully exploited and generalized.)

Equivalent passband

Schade's equivalent passband (N_e) is an index of image quality that appears in one form or another in many imaging applications. It can be written in two dimensions as the following:

$$N_e = \int_{-\infty}^{\infty}\int_{-\infty}^{\infty} \mathrm{MTF}^2(f_x,f_y)\,df_x\,df_y. \qquad (1)$$

It is the volume under the surface formed by the squared modulus of the transfer function, normalized to unity at zero spatial frequency.

In the following we will be recommending this quantity (actually, its reciprocal) as a practical form to which the more complete MTF might be reduced for the sake of broader utility among users of radiographic systems.

Of the many indexes that have been suggested for imaging systems, we are suggesting this form for the following reasons:

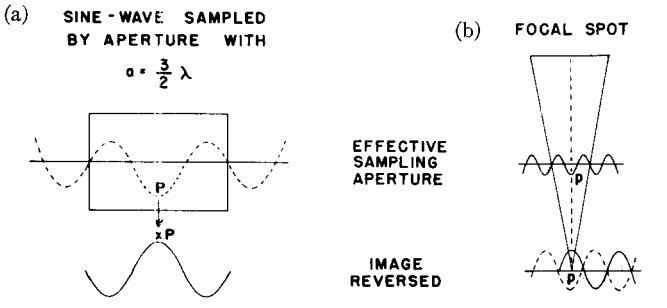

FIG. 11. (a) The averaging process of a sampling aperture, considered in detail, explains the phenomenon of *spurious resolution* (180° phase shift). (b) Example of the focal spot as a sampling aperture: A uniform focal spot gives an image at a point which represents an average over its effective aperture in the sampling (or object) plane.

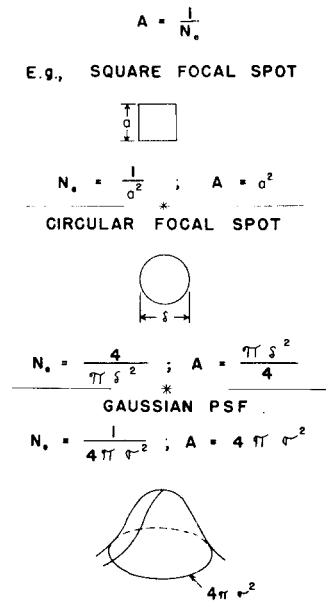

FIG. 12. The equivalent passband in two dimensions and its reciprocal, the effective sampling aperture, for three simple examples.

(1) It is approximately proportional (in its one-dimensional version) to the quantity called *acutance*, that is, the rms gradient of the image of an edge exposure.[13–16] This quantity has been found to be one of the best correlates of the subjective impression of "sharpness."[13]

(2) It gives rise to an effective sampling aperture with a straightforward interpretation. This is accomplished by taking its reciprocal. That is to say, the greater the volume under the squared MTF surface, the smaller the effective sampling aperture, or average blur size, and vice versa.

In one dimension this quantity (effective sampling aperture) is approximately proportional to the effective width of an edge transition, a classical measure of sharpness[17] which correlates well with "the general subjective impression of image sharpness in both television and photographic images"[18] which include the range of spatial dimensions encountered in radiography.

(3) We will see that the effective sampling aperture can be used in a simple approximate rule for combining the effects of focal spots and intensifying screens, and other imaging components.

Many other figures of merit for grading imaging systems can compete with the effective-sampling-aperture concept as described in item (2) above [e.g., full width at half maximum of the line-spread function, spatial frequency at 50% MTF, the integral of the MTF, etc.[19]]. However, as pointed out by Schade,[18] why have *several* measures when *one* can serve all of the above functions, as well as have utility as the proper bandwidth measure for evaluation of noisy systems (see Ref. 12; we will treat this concept in our future applications for noisy systems; Ref. 20 indicates the direction to be taken).

Further, if our future efforts with Fourier optics are successful, this quantity would be straightforward to measure directly since the quantity to which any detecting device (film, photocell, etc.) placed in the far-field diffraction pattern would respond is in fact the squared modulus of the Fourier transform.

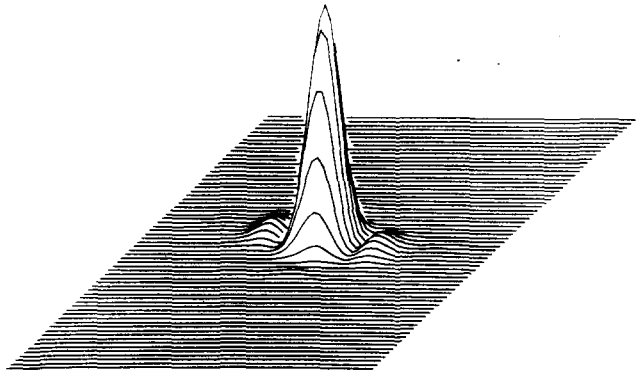

FIG. 13. The square of the function shown in Figure 6(c). The side lobes contain less than 10% of the entire volume under the squared MTF surface.

Let us consider a few ideal applications of these concepts before moving on to the practical applications. In Fig. 12 three examples of sampling apertures are displayed. In the first two simple cases (namely, a square and a circular aperture), if one calculates the equivalent passband in two dimensions according to the above prescription and takes its reciprocal, the effective sampling aperture, one arrives at the results expected naturally, since the blur or smear area of a uniform aperture is just the aperture area (an obvious application here is a scanning densitometer aperture; for the case of focal spots, the results hold in the plane of the focal spot—they must be scaled to the object plane as suggested earlier and will be done below). A more interesting case is that of a focal spot, or other PSF, with a Gaussian distribution with standard deviation σ. In this case the equivalent passband is equal to $1/(4\pi\sigma^2)$; this makes the effective sampling aperture equal to $4\pi\sigma^2$. This is to say that in our treatment the average blur size for a Gaussian smear is a circle with a radius equal to 2σ, or a diameter equal to 4σ. (When this calculation is done in one dimension, the resulting diameter is 3.5σ; this number may be compared with an experimental result of fitting one-dimensional focal spot data by a Gaussian with $3\sigma = a$, the focal spot width.[21])

Now let us consider the case of a realistic focal spot. The absolute square of the Fourier transform of the focal spot of Fig. 6(a) is shown in Fig. 13. The equivalent passband is the volume under this surface. The volume consists of a major central lobe, together with side lobes. The first side lobes correspond to the regions of spurious resolution. Spurious resolution is a complicated phenomenon not easily categorized as to "goodness" or "badness." More generally it gives rise to a degradation in edge sharpness; but there are cases where it might tend to enhance detectability, e.g., in the case of objects smaller in size than the spread function,[22] and, of course, in the case of certain frequencies in a spoke target. We have decided tentatively to neglect the volume under the side lobes in calculating the equivalent passband. This means that a system is weakly penalized for spurious resolution. [If one were to neglect this penalty and use the volume under the entire MTF-squared surface, Fourier analysis would be unnecessary in this application. This volume is related to the volume under the intensity-squared distribution in coordinate (as opposed to frequency) space by Parseval's theorem, often interpreted as an energy conservation theorem.]

The above ambiguity is only a minor consideration, in our context, however: We have observed no cases where the volume under the side lobes exceeds 10% of the entire volume under the squared MTF. We will see later that this is within the limits of error of our technique.

The effective sampling aperture or average blur size is then found as the reciprocal of this number. It can be expressed as an area, or one can state the diameter of the equivalent circle with the same area. We have done this for a number of x-ray tube focal spots which we have studied in our laboratories. Before presenting the results, we will review several other criteria or rules for prescribing the effective size of focal spots. Then we will be able to compare the results from various prescriptions.

The prescription from ICRU document 10f[23] includes making a pin-hole radiograph of the focal spot and subjectively measuring its outside dimensions with a 5× magnifier. The long dimension is then multiplied by a ("tentative") factor of 0.7 to take into account that the intensity is much greater in the center than near the edges for typical distributions. We have followed this rule and obtained the effective area of the focal spot. This number was then converted to the diameter of the equivalent circle for comparison with our approach (Fig. 14-I).

Another prescription makes use of the disappearance frequency mentioned earlier. There are several versions of this rule. The version employed by Gopala Rao[24] and others is to express the focal-spot size in terms of the dimension of a uniform distribution which would give the same disappearance frequency, or what we refer to as the "first blur." For example, if one uses a geometry with a magnification of 2×, then the effective focal spot size is given by $2/f_0$, where f_0 is the disappearance frequency of a bar or spoke target (the general rule is $M/(M-1)f_0$ where M is the magnification

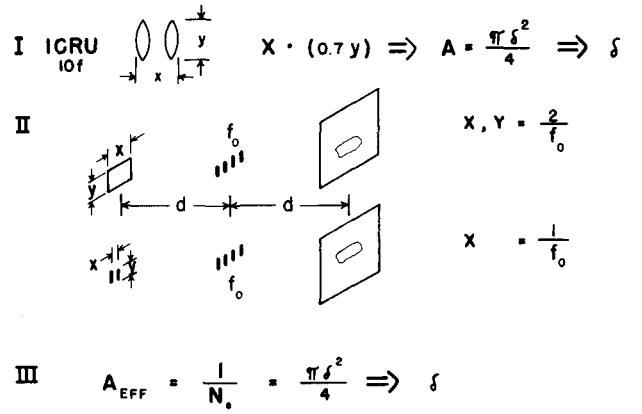

FIG. 14. Three prescriptions for obtaining the "size" of a focal spot: (I) direct measurement according to ICRU document 10(f); (II) (a) using the disappearance frequency to determine the equivalent rectangle; (b) using the disappearance frequency to determine the spacing of the equivalent two-line source; (III) the effective aperture rule introduced in this paper. In each case, we calculate an area from these numbers and reduce this to the diameter of the equivalent circle.

employed). In general, this number depends on the orientation of the bar pattern. In applying this rule we took disappearance frequencies perpendicular and parallel to the tube axis to calculate values of x and y, multiplied these values to form an area, and reduced this to the diameter of the equivalent circle.

A different version of this rule takes into account the double-hot-spot form of the x-ray intensity distribution. Bookstein[25] expresses the focal-spot size in terms of the dimension of separation of a double-line source which would give the same disappearance frequency. For the magnification of 2× in the example above, his effective focal spot size is then given by $1/f_0$. That is to say, a double line source must have one-half the dimension to have the same cut-off frequency as the uniform source (Fig. 14-II).

The foregoing is another way of saying that the disappearance frequency rule is heavily model dependent in its application, and so can be subject to misinterpretation. In fact, for a Gaussian blur function there is no well-defined disappearance frequency: The contrast transfer function itself goes to zero as a Gaussian without the dramatic zero cross-over. In this case, the rule would be very difficult to apply.

In our comparisons we have chosen to apply the former version, judging that the latter version can give the more misleading result. In principle, if one prefers to use the disappearance frequency, the safest route is not to convert this to a dimension, but merely to state the frequency and the magnification.

The final prescription used in our comparisons is the one we have introduced in this paper, namely, finding the effective sampling aperture (or average blur size), as the reciprocal of the equivalent passband (volume under the central lobe of the squared MTF). This number is then converted to the diameter of the equivalent circle. In other words, a non-uniform, two-dimensional source distribution has been reduced to a uniform circular distribution which gives rise to the same "sharpness" or "acuteness" on the average in the sense of *equivalent* equivalent passbands (*sic*) (see Fig. 12).

Type	Nominal	ICRU[a,b] (10 f)	First Blur[a]	Eff. Apert.[a,c]
C.D.				
3ϕ L	2.0 mm	3.2 mm	3.1 mm	2.9 mm
200 mA	2.0	2.8	3.1	3.0
3ϕ L				
1200 mA	2.0	3.1	3.7	3.7
3ϕ S				
80 kV	1.0	1.5	1.7	1.7
3ϕ S				
150 kV	1.0	1.5	1.7	1.7
D.U.I.	1.0	1.9	1.7	1.8
Exp. D.U.I.	1.0	1.7	1.3	1.7

[a] Diameters; square would have edge 11% smaller.
[b] Subject to 10% error due to pinhole smearing.
[c] Subject to 15% error due to pinhole and digital filter smearing.

FIG. 15. Results of applying the prescriptions of Fig. 14 to x-ray tube focal spots in our laboratory: Capacitor discharge unit; 3-phase unit, large spot, 200 mA and 1200 mA; 3-phase unit, small spot, 80 kV and 150 kV; "Diagnostic Unit I," a single-phase unit; and "Experimental Diagnostic Unit I," also a single-phase unit. The error cited is the total uncertainty in the measurement.

Quantitative results for focal spots

Figure 15 contains the results of our study of several x-ray tube focal spots in our laboratories. The first column gives the type of generator; the second column gives the nominal size of the focal spot; the next three columns give the effective diameters of these focal spots calculated according to the three prescriptions just presented. The most obvious comparison that can be drawn is this: All of the prescriptions give sizes significantly greater than the nominal size of the focal spot. Next, one can see that the ICRU rule and the disappearance frequency rule do not track—one rule can give values larger or smaller than the other. The comparison of the last two columns is quite striking. They agree quite well, up to the last entry. This case makes an interesting comparison.

The MTF for the last focal spot in the table is shown in Fig. 5(c). In the direction coming toward the front of the picture, notice how the MTF comes plunging toward zero, but hangs up at a low value for an equal period, then passes through zero. The disappearance frequency rule overrates this focal spot by treating the MTF as if it were to come down to its zero crossing at values higher than in fact it does. The effective sampling aperture gives it credit for only as much MTF as it in fact has. For this reason we feel that it is a more precise criterion. However, it appears that, at least in our laboratory, this is a peculiar case; so the disappearance frequency rule has a rather wide range of utility, especially as a more straightforward field type of test (version due to Rao).

A final point of comparison that has been noted also by Gopala Rao and Bates[5] is the insensitivity of focal spot size to tube voltage (at least for the voltages studied); on the other hand there is a significant increase in size with tube current—the so-called "bloom" which is familiar to many workers in the field (see Figs. 16 and 17).

V. Systems applications

The effective sampling aperture approach leads quite naturally into a very useful approximate tool for cascading imaging components into a system. Earlier we pointed out that the effective aperture for a Gaussian component is equal to $4\pi\sigma^2$. If one is dealing with components that can be considered to have approximately Gaussian MTFs, a simple law of combination results. Recall that in cascading Gaussians one has the simple sum of squares law: $\sigma_{\text{total}}^2 = \sigma_1^2 + \sigma_2^2$. This is to say that if one has the effective aperture parameters for two components that are to be cascaded into a system, to obtain the effective aperture of the system, merely proceed as in addition (i.e., add).

The Gaussian assumption turns out to be quite reasonable for several broad classes of imaging components. Bruce Johnson[26] has pointed out that many MTFs may be fit

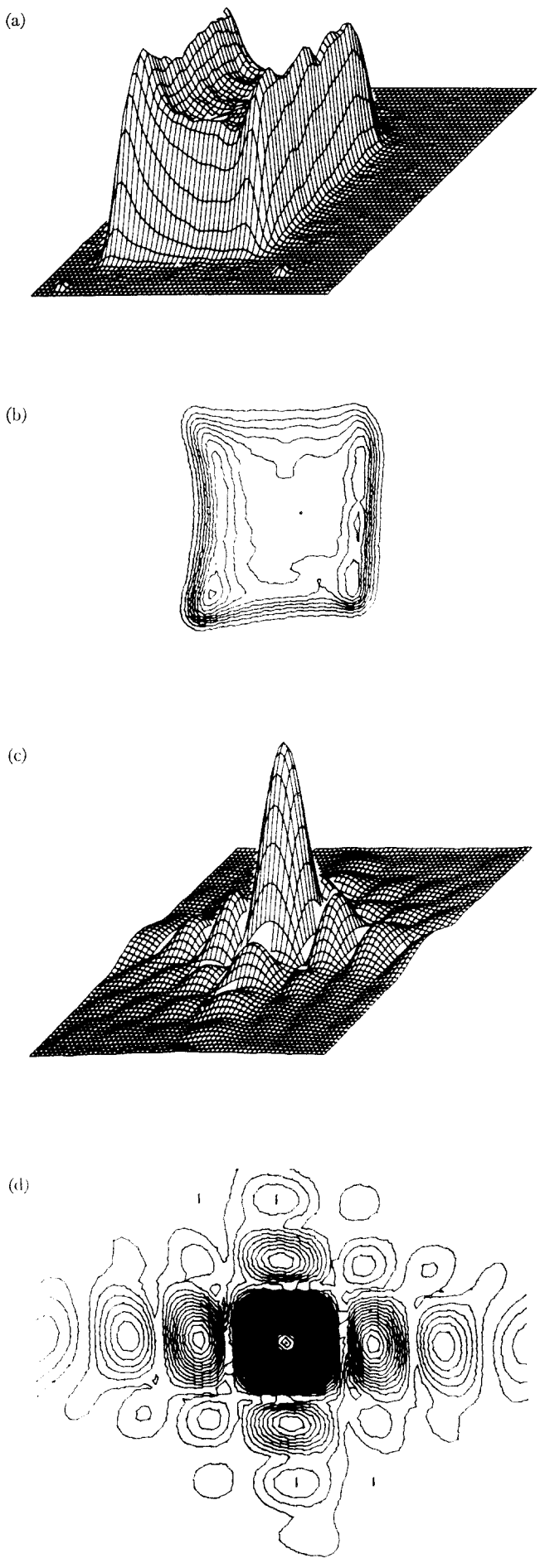

with an expression of the form

$$\mathrm{MTF}(f)=\exp[-(f/f_c)^n], \tag{2}$$

where f_c is a width parameter (broadly speaking, a cut-off frequency) and n is, of course, the power of an exponential. When this latter parameter is equal to 2, the function is a Gaussian. He has introduced a graph paper for plotting MTFs from which these parameters can be read off immediately. X-ray intensifying screens seem to be fit over a wide range of frequencies with a power n equal to a value between 1.5 and 1.8. Other workers have had success in fitting image intensifier MTFs with Gaussians, and similarly for x-ray tube focal spots.[21] The latter becomes even more reasonable if the portions of the MTF after the disappearance frequency are discarded. It is interesting that motion unsharpness has an MTF which is analogous to an idealized focal spot MTF so it also can be placed in this category.

This means in practice that one might find the equivalent passband or volume under the squared MTF surface as a very useful tool in the form of its reciprocal, the effective sampling aperture. A very broad class of component apertures can then be readily combined into an overall system effective aperture. This is a simple addition law if we are concerned with apertures or blurs in terms of their areas A (sum of squares law); or a simple triangle addition law if we are concerned with combining effective diameters of blur functions δ (Fig. 18):

$$A_{\text{system}}=\textstyle\sum_i A_i \text{ or } \delta_{\text{effective}}=(\sum_i \delta_i^2)^{\frac{1}{2}}. \tag{3}$$

Many *ad hoc* rules for combining unsharpnesses have been utilized in imaging systems for decades.[17,27] The present one comes out of the above treatment in a natural way with a mild assumption and a straightforward prescription. We will try the pudding in a moment. Let us first apply this scheme to the case of an x-ray tube focal spot and x-ray intensifying screen in cascade.

This problem becomes quite straightforward under the above convention, namely, specifying the effective aperture of the focal spot *in its own plane*, A_{FS}, and the effective aperture of the intensifying screen *in its own plane*, A_S. Then these quantities need only be referred to the object plane for a given condition of magnification (the object plane is the meaningful plane of interest since this is where we want the resolution). The geometry for this scaling is shown in Fig. 19. Primes denote the quantity after scaling to the object plane. This figure brings out the symmetric roles played by the screen and the focal spot.

FIG. 16. Intensity and MTF distributions for three-phase unit, large spot, 200 mA (Fig. 16) and 1200 mA (Fig. 17). Pin-hole radiographs for these cases were made under condition of 1:2 magnification. For other parameters see captions for Figs. 4–6. Effect of increase in current is manifested in "bloom" (increased cross section) and intensification of double hot-line effect. Distribution of Fig. 16 approaches rectangular uniform distribution; distribution of Fig. 17 is a compromise between the latter and the simple double-line source. Their MTF contours may be compared with diffraction patterns associated with the classical extreme cases.

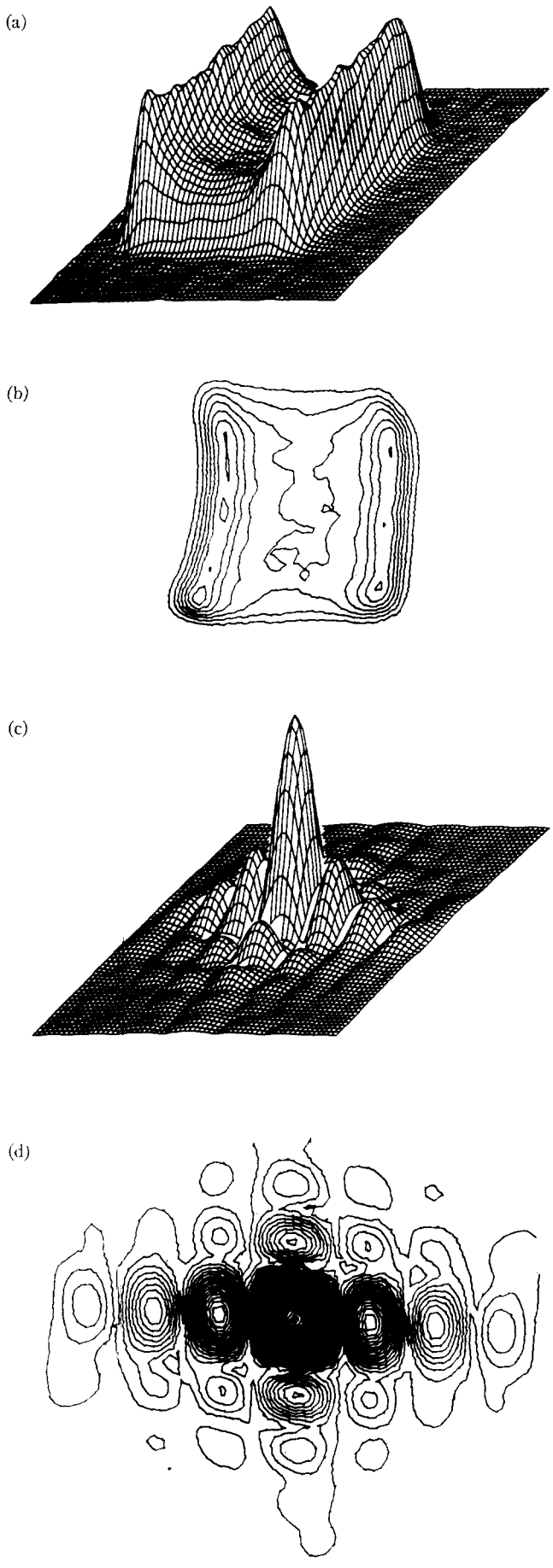

FIG. 17. See Fig. 16 caption for discussion.

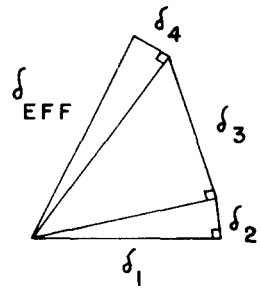

FIG. 18. The sum-of-squares rule applies to the cascading of Gaussian blurs; the linear dimensions of the blurs add up according to a simple triangular addition rule. Cascading of blurs due to focal spot, motion, image intensifier, etc. can be calculated approximately from a polygon of triangles as shown here.

The next step is to write the effective aperture of the system (referred to the object plane) as the sum of the effective apertures of the components. Referring to Fig. 19 and applying the addition law in the plane of the object leads to the result

$$A_{\text{object}} = A_{\text{FS}}' + A_{\text{S}}' = M^{-2}[(M-1)^2 A_{\text{FS}} + A_{\text{S}}] \tag{4}$$

for the effective sampling aperture or blur size in the plane of the object, A_{object}. Here we have written the ratio $(d_1+d_2)/d_1$, the system magnification, as M. If this expression is differentiated with respect to d_1 (or M, say), we find that it has a minimum at a magnification

$$M_{\text{optimum}} = 1 + A_{\text{S}}/A_{\text{FS}}. \tag{5}$$

This gives the magnification for the best resolution, in the sense of "sharpness" as defined above, in the context of this simplified model. (At the time of this writing we have found that these equations already exist in the literature[28] in almost the same form as given here, but from the lack of reference to them it appears that they have not received widespread attention.)

We have plotted the above equations in Fig. 20 for a variety of situations that may be encountered in radiography. There are six plots for six focal spots ranging from 2.0 mm to 0.05 mm (50 μm). The focal spots are treated as uniform squares with edge a equal to the number shown;

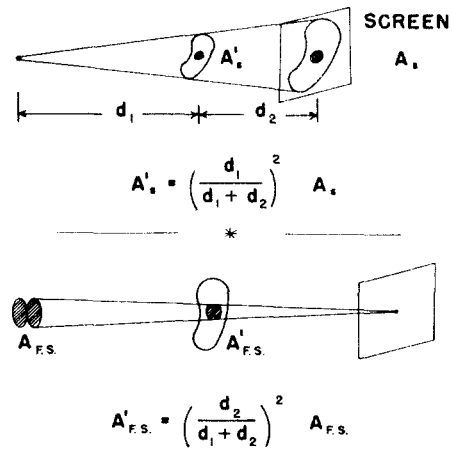

FIG. 19. The geometry for combining focal spots and screens: A is the effective aperture in the plane of the respective component; A' is the effective aperture referred to the object plane. The symmetry of the roles of focal spot and intensifying screen is made obvious in this sketch.

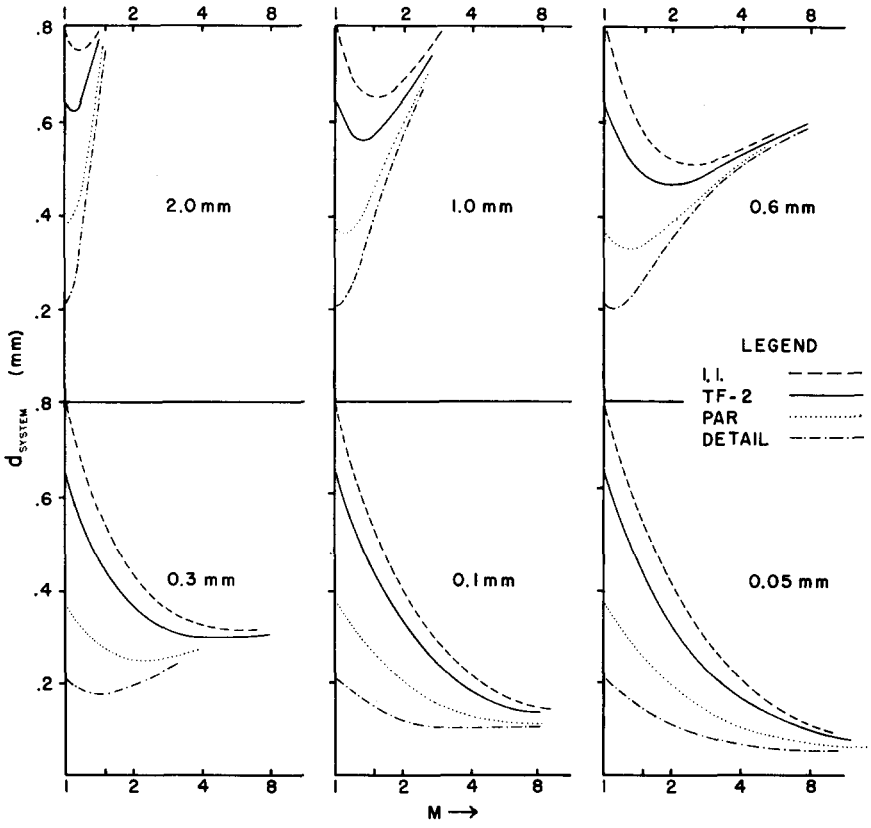

FIG. 20. Graphs of Eqs. (4) and (5) for the case of six ideal focal spots: 2.0-mm square down to 50-μm square (assumed to have uniform distributions) and three commercially available screens and a fictitious image intensifier. M is the system magnification ($M = 1$ means thin object against cassette), and d is the system effective blur diameter in the object plane (smaller values of d corresponding to better average resolution).

this means they have an effective sampling aperture equal to a^2 (for a square focal spot, volume of squared MTF outside of the central lobe is less than 5% of the total; this difference is neglected). A family of four curves for four image receptors is shown for each focal spot: curves for three x-ray intensifying screens, namely, Detail, Par, TF-2, and a fictitious image intensifier tube (I.I.). The effective apertures for the Par and TF-2 screens were calculated from exponential parameter fits given by Doi[29]; for Detail screens, MTF data given by Morgan, *et al.*[30] and Rossman[31] were numerically integrated and averaged; the effective aperture for I.I. was arbitrarily set equal to twice the result for Par.

The curves show the dependence of the effective sampling diameter (i.e., effective aperture treated as a circle with the diameter shown) of the system d_{system} referred to the object plane as a function of magnification M. The smaller the value of d_{system}, the smaller the average blur, the better the resolution, in the above sense, and vice versa.

Referring to the equation plotted, we can notice several general characteristics of these curves. First, for $M=1$, of course, the focal spot does not enter, and all the blurring is due to the screen. The curves all pass through a minimum or optimum resolution, as mentioned above (an interesting kind of synergism, if you will, where the system is better than its weakest link; see Ref. 21 for an example that is an interesting exception). Finally, they go asymptotically (for large M) to a value that is completely determined by the effective aperture of the focal spot (careful observation will show that the asymptotic value is 11% larger than the focal spot dimension—this is due to our reducing the square to a circle of equivalent area—its diameter is 11% larger than the edge of the square).

Next, some particulars: Notice how for the larger (2.0 mm and 1.0 mm) focal spots, a slight amount of magnification quickly deteriorates sharpness for the slower systems. The results for the 2.0 mm focal spot agree quite well with results of a more complete calculation published by Gopala Rao.[32] (It should be noted that this curve applies to an ideal 2-mm focal spot; in practice a nominal 2-mm focal spot is significantly larger—see Fig. 15.)

In the case of the 0.6 mm focal spot, and in the range of general diagnostic application (M = 1.0–1.5 or so) there is no loss of resolution—rather generally an increase—with magnification for the Par and TF-2 screens (compared to a magnification of one). Such a focal spot will improve the resolution of an image intensifier up to at least a magnification of 2×.

More complete calculations of the above sort have been carried out by Gopala Rao, *et al.*[33] and by Doi and Rossmann.[34] The trends of our simple model follow the indications of the former paper. The latter authors have given trade-off points of fast systems with magnification against slower systems without magnification. The simplified treatment of our paper agrees generally to within 80% to 100% of their numbers. (Their results include the dependence on object spectra; see also Ref. 21.)

There are several exceptions where our curves just miss giving rise to a trade-off point. If one allows the present curves to have a small width, e.g., introducing error bars due to the many variables of a practical situation (see

Ref. 35 where this is done), then our results and those of Ref. 34 agree very well.

Our curves are in general agreement with the experimental findings of Eisenberg, *et al.*[35] and also Hollander, *et al.*[36] The latter workers however find it disadvantageous to use magnification with the 0.1 mm focal spot and detail screens on the basis of the resolution of a bar target. We seriously doubt whether judgements of the overall utility of magnification radiography should be made on the basis of the disappearance frequency of a bar target. In principle, magnification will decrease the value of the disappearance frequency of a focal spot and increase the "cut-off" frequency of a screen. If the screen cannot resolve the focal spot disappearance frequency, one will judge magnification to be advantageous. Once the screen can resolve the focal-spot disappearance frequency, one will judge magnification to be disadvantageous. This can easily happen with detail screens, giving a bad judgment about their utility. Yet it is quite possible that the *average* detail perceptibility of diagnostic information can increase while the cut-off frequency decreases. These questions will have to be resolved in clinical or simulated clinical situations.

Cautions

The reader familiar with the practical radiographic situation will no doubt be concerned with the complications introduced into the above simplified picture by such effects as off-focus radiation, scatter, and its reduction by grids and by the air-gap technique, etc. Our treatment above considered ideal focal spots and real focal spots collimated to eliminate most off-focus radiation; we have neglected the effects of scatter.

We have, however, made measurements of the off-focus radiation emitted by the tubes in our laboratory. The extremes are represented by a tube in which off-focus radiation was just a few percent of the total radiation emitted by the tube, and a tube in which it amounted to 25% of the total radiation emitted (and typically spread out over an area larger than the focal spot itself by one or two orders of magnitude). These findings are in basic agreement with a more extensive study carried out by Gopala Rao.[37] The effect is a general increase in background analogous to scatter. In turn, this affects the values of the unnormalized MTF close to zero spatial frequency by the same percentage. When the MTF is then renormalized to 100% at zero frequency, the entire MTF curve is lowered. In the above treatment (and, of course, even intuitively) such a focal spot will look significantly larger than predicted by any treatment that neglects the off-focus radiation. In fact, this can amount to an increase of 50% in the effective linear dimension of a focal spot. This effect is not noticed with a spoke or bar target since the overall contrast reduction does not affect the disappearance frequency (when the off-focus radiation is spread over a large area). A convention for specifying focal-spot size, such as that suggested above, will then have to include additionally some measure of the extent and intensity of off-focus radiation. This is a matter for future study. It should be noted, however, that it is possible to significantly reduce this effect (that is to say, exposure which produces almost no useful image, rather, a degradation of the image) by proper collimating fingers at the tube.

The problem of scatter is somewhat analogous to the question above. Scatter may be thought of roughly as producing a uniform increase in the background level of exposure. This affects the value of the unnormalized system MTF at zero frequency. Again, when renormalizing to 100% at zero frequency, the entire MTF is lowered by a constant fraction; this of course raises the system effective sampling aperture. The problem in introducing this effect into the above treatment is this: When magnification is used, one in effect is using the so-called "air-gap technique" which reduces the recording of scatter. This is a function of the object and the air-gap separation; and the latter translates into magnification. So the resulting shift of the system effective-aperture curves is not a constant; the effect is more dramatic for smaller values of magnification than at greater values, where the effect of the air-gap tapers off to a constant—all of which is object dependent.

We believe that the above question can be parametrized, but the problem is still outstanding. Thus this word of caution in using the conventions suggested in this paper. When grids are employed, much of this ambiguity is removed.

Conclusion

We have introduced the concept of effective sampling aperture (or average blur size). If we can establish a convention for measuring this quantity—either from measured MTF data, or more straightforwardly by doing photometry with a simple laser–lens system—a parameter can be made available to a user to help him judge the quality of an imaging component with regard to "sharpness." To the extent to which his component MTFs can be approximated by Gaussians (generally fairly reasonably), he can employ a simple rule of thumb for combining component parameters to estimate system performance.

Our final results have a total uncertainty of less than 15%, and their predictive ability may be at least as good as 80% for a wide class of situations. We believe that these numbers are very good in a field (x-ray tube focal spots) where the latitude of specification currently tolerated is about 100%, i.e., a factor of 2.

The treatment given was for situations that are not noise limited. We are currently working on an extension of this treatment to the case of noisy images.

Acknowledgments

The results reported here were made possible by the efforts of our Systems Engineer, Malcolm Bruce, and Systems Programmer, William Pakenas. Our Fourier optics apparatus was assembled by Irv Coates; our illustrations are the work of Dean Elbert. We gratefully acknowledge the part played by these members of a project that was essentially a team effort.

We have benefited from helpful discussions with David J. Goodenough and Kunio Doi, and are grateful to the latter as well as to Ralph Shuping and Professor Moses A. Greenfield for bringing to our attention some of the earlier work in magnification techniques whose indications run parallel to those at the end of this paper.[38–40]

[1] R. H. Morgan, L. M. Bates, Gopala U. V. Rao, and A. Marinaro, Amer. J. Roentgenol. **92**, 426 (1964).

[2] K. Rossmann, "Image quality and patient exposure," Current Probl. Radiol. **II** (March–April 1972) and references therein.

[3] *Diagnostic Radiologic Instrumentation—Modulation Transfer Function*, edited by R. D. Moseley and J. H. Rust (Thomas, Springfield, IL, 1965).

[4] K. Doi, Amer. J. Roentgenol. **94**, 712 (1965).

[5] Gopala U. V. Rao and L. M. Bates, Phys. Med. Biol. **14**, 93 (1968).

[6] N. C. Beese, Rev. Sci. Instrum. **8**, 258 (1937).

[7] E. N. C. Milne, CRC Critical Rev. Radiol. Sci. **2**, 269 (1971).

[8] J. E. Gray, M. P. Capp, R. R. Shannon, and F. R. Whitehead, Proc. Soc. Photo-optical Instrumentation Eng.—Appl. Opt. Instrum. Medicine **35**, 95 (1973).

[9] M. C. Bruce, K. E. Weaver, R. F. Wagner, and W. P. Pakenas, Q. Bull. Amer. Assoc. Phys. Med. **7**, 90 (1973).

[10] J. W. Goodman, *Introduction to Fourier Optics* (McGraw-Hill, San Francisco, 1968).

[11] O. H. Schade, J. Soc. Motion Pict. Telev. Eng. **58**, 181 (March 1952).

[12] R. H. Morgan, Amer. J. Roentgenol. **93**, 982 (1965). See also p. 85 of Ref. 3 for a discussion of this article.

[13] G. C. Higgins and L. A. Jones, J. Soc. Motion Pict. Telev. Eng. **58**, 277 (1952).

[14] O. H. Schade, J. Soc. Motion Pict. Telev. Eng. **64**, 593 (1955).

[15] P. G. Roetling, E. A. Trabka, and R. E. Kinzly, J. Opt. Soc. Amer. **58**, 342 (1968).

[16] R. F. Wagner and K. E. Weaver, Proc. Soc. Photo-opt. Instrum. Eng.—Appl. Opt. Instrum. Medicine **35**, 83 (1973).

[17] R. Halmshaw, *Physics of Industrial Radiology* (Heywood Books, London, 1966), p. 183.

[18] O. H. Schade, Appl. Opt. **3**, 17 (1964).

[19] K. G. Birch, "Survey of OTF based criteria used in the specification of image quality" (Natl. Phys. Lab. Teddington, Engalnd, 1969); Clearinghouse for Fed. Sci. Tech. Info., Springfield, VA, No. 70-21982.

[20] R. F. Wagner and D. J. Goodenough, "The Figure of Merit and Other Figures with Merit," in *Methods for Evaluating Radionuclide Imaging Procedures: A Critique* (Society of Nuclear Medicine—Mid-Winter Symposium, January, 1974), to be published.

[21] K. Doi and K. Sayanagi, Jap. J. Appl. Phys. **9**, 834 (1970).

[22] P. F. Friedman and R. H. Greenspan, Radiology **92**, 549 (1969).

[23] International Commission on Radiological Units and Measurements, 1962 Report. National Bureau of Standards Handbook 89, 1963.

[24] Gopala U. V. Rao, Amer. J. Roentgenol. **111**, 628 (1971).

[25] J. J. Bookstein and W. Steck, Radiology **98**, 31 (1971).

[26] C. B. Johnson, Electro-Opt. Sys. Des. **4**, 22 (Nov. 1972).

[27] W. J. Meredith and J. B. Massey, *Fundamental Physics of Radiology* (Williams and Wilkins, Balitmore, MD, 1968), p. 261.

[28] K. Sayanagai, "Consideration of non-linearity in image transfer systems," in Moseley and Rust, *Television in Diagnostic Radiology* (Aesculapius Publ., Birmingham, AL, 1969), p. 406.

[29] K. Doi, "Investigation of Radiological Image." Proc. Radiat. Image Inf. **2**, 264 (1969); cited in D. J. Goodenough "Radiographic Applications of Signal Detection Theory," Ph.D. thesis (Univ. Chicago, Chicago, IL, 1972), p. 96.

[30] These data are found in an extended version of Ref. 1, submitted as a report for Research Contract SAph76496, Division of Radiological Health, U.S. Public Health Service.

[31] K. Rossmann, A. G. Haus, and G. D. Dobben, Radiology **96**, 361 (1970).

[32] Gopala U. V. Rao, Amer. J. Roentegenol. **112**, 812 (1971).

[33] Gopala U. V. Rao, R. L. Clark, and B. W. Gayler, Appl. Radio. **2**, (No. 1), 37; **2**, (No. 2), 25 (1973).

[34] K. Doi and K. Rossmann, Q. Bull. Amer. Assoc. Phys. Med. **6**, 195 (1972).

[35] H. Eisenberg and W. P. Holland, *Magnification Arteriography with Grid-biased Focal Spot X-ray Tubes, A Cathode Press Supplement* (Machlett Laboratories, Inc., Stanford, CT, 1972).

[36] B. A. Hollander, S. K. Hilal, and W. B. Seaman, Radiology **103**, 667 (1972).

[37] Gopala U. V. Rao, "Influence of focus and off-focus radiation on radiographic detail (modulation transfer function) and patient exposure in diagnostic radiology" (a report on work carried out under Contract number SAph76496 between the Johns Hopkins University and the Division of Radiological Health, U.S. Public Health Service).

[38] S. Takahashi, T. Sasaki, S. Sakuma, and K. Tobita, "X-ray television macrofluoroscopy," in Moseley and Rust, *Television in Diagnostic Radiology* (Aesculapius Publ., Birmingham, AL, 1969), p. 121.

[39] A. Nemet and W. F. Cox, Br. J. Radiol. **29**, 335 (1956).

[40] G. C. E. Burger, B. Combee, and J. H. van der Tuuk, Philips Tech. Rev. **VIII**, 321 (1946).